

Cite this: *Chem. Sci.*, 2025, **16**, 6957

All publication charges for this article have been paid for by the Royal Society of Chemistry

Received 11th February 2025  
Accepted 12th March 2025

DOI: 10.1039/d5sc01068c  
[rsc.li/chemical-science](http://rsc.li/chemical-science)

## Introduction

Sulfoximines have gained increasing popularity in pharmaceutical and agrochemical research as versatile isosteric replacement of sulfones, sulfonamides, carbonyl compounds, amines or alcohols, among others (Fig. 1a).<sup>1</sup> These compounds possess interesting properties, such as high chemical stability, increased solubility in water<sup>2</sup> and multiple hydrogen bond donor/acceptor sites. Further, the N-atom adds value to the structure by adding intrinsic chirality, with the possibility of exploring the 3D-chemical space with defined exit vectors. On the other hand, replacing hydrogen atoms with highly electronegative fluorine atoms is a common strategy to modulate properties, reactivity and conformations of molecules.<sup>3</sup> In this regard, F-containing sulfoximines have found applications as key elements in bioactive compounds (Fig. 1a) or functional materials.<sup>4</sup> However, general synthetic methods for the preparation of these classes of fluorinated compounds are still largely underdeveloped.<sup>4a</sup> In recent years, we undertook a research line for the development of effective methodologies to achieve the construction of F-

containing sulfoximines **1** (Fig. 1b).<sup>5</sup> Interestingly, these structures **1** have exhibited synthetic versatility in photoredox catalytic systems,<sup>6</sup> with reactivity influenced by the *N*-substitution pattern (Fig. 1b). On one hand, *N*-tosyl and *N*-triflate sulfoximines (**1**, *X* = Ts or Tf, respectively) have been used as fluoroalkyl radical sources (pathway i).<sup>7</sup> Here, a single electron transfer (SET) process from an excited photocatalyst to **1** triggers a C–S bond homolytic cleavage, while releasing fluorinated C-centered radicals (**RF**<sup>·</sup>). These radicals have been subsequently engaged in radical additions with alkenes **3**, ultimately forming fluoroalkyl products **4**. In these strategies, the sulfoximine unit is not incorporated into the final target **4** but only serves as an auxiliary for the generation of reactive fluoroalkyl radicals. On the other hand, the group of Magnier utilized *N*-chloro substituted sulfoximines (**1**, *X* = Cl) in photoinduced SET reductions (pathway ii), promoting N–Cl homolytic bond scission while generating the corresponding *N*-sulfoximidoyl radical **2**.<sup>8</sup> The *N*-centered radical **2** has also been successfully engaged in radical addition processes with alkenes **3**, offering a straightforward access to *N*-alkylated fluorinated products **5**. Aiming at identifying novel reaction manifolds for **1**, while addressing the increasing demands of fluorinated sulfoximines, we wonder whether an alternative scission pathway could be promoted to access difluoroalkyl sulfoximine radicals **6** (pathway iii), for which there are currently no available methods. Success in this endeavor will offer new avenues for the synthesis of CF<sub>2</sub>-sulfoximines *via* radical chemistry, while allowing the generation of novel F-containing building blocks.<sup>9</sup>

Herein, we detail a mild organophotoredox strategy that gives access to unprecedented difluoroalkylsulfoximine radicals **8**, while engaging them in divergent reaction manifolds (Fig. 1c). Our approach is based on the use of

<sup>a</sup>Department of Chemical Sciences, University of Padova, Via Francesco Marzolo 1, 35131, Padova, Italy. E-mail: [sara.cuadros@unipd.it](mailto:sara.cuadros@unipd.it); [luca.dellamico@unipd.it](mailto:luca.dellamico@unipd.it)

<sup>b</sup>Institut Lavoisier de Versailles, Université Paris-Saclay, 45 avenue des Etats-Unis, 78035 Versailles, France. E-mail: [emmanuel.magnier@uvsq.fr](mailto:emmanuel.magnier@uvsq.fr)

<sup>c</sup>Université de Tours, Faculté des Sciences et Techniques, 37200 Tours, France

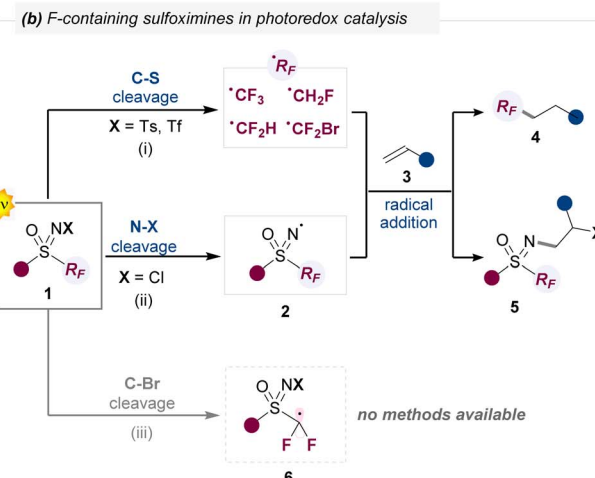
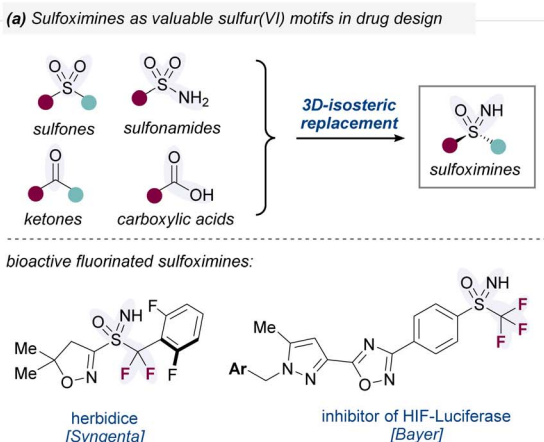
<sup>d</sup>Department of Chemistry, Life Sciences and Environmental Sustainability, University of Parma, Parco Area delle Scienze 17, 43124, Parma, Italy

<sup>e</sup>Aix Marseille Univ., CNRS, ICR, 13013 Marseille, France

† Electronic supplementary information (ESI) available. CCDC 2364218. For ESI and crystallographic data in CIF or other electronic format see DOI: <https://doi.org/10.1039/d5sc01068c>

‡ These authors contributed equally.





(c) This work: light-driven radical difluorosulfoximation processes

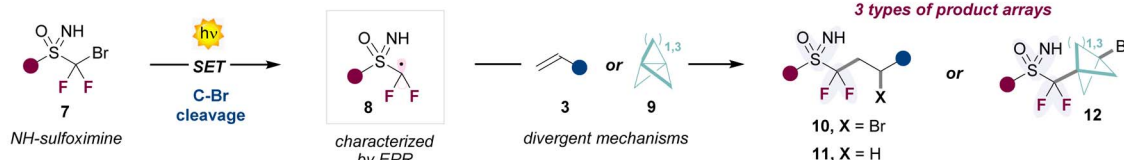


Fig. 1 (a) Application of sulfoximines in drug design and examples of biologically active fluorinated sulfoximines. (b) Available reactivity pathways for fluorinated *N*-substituted sulfoximines 1, under photoredox catalyzed conditions. (c) This work: light-driven difluorosulfoximation of unactivated alkenes 3 and propellanes 9. PC: photocatalyst; SET: single electron transfer.

bromodifluoroalkyl NH-sulfoximines 7, which upon photoinduced SET, undergo preferentially C-Br homolytic cleavage to produce the target radicals 8. These intermediates successfully engage in different radical addition processes with unactivated alkenes 3 and propellanes 9, either *via* atom-transfer radical addition (ATRA) or hydrofunctionalization mechanisms.<sup>10</sup> Using this divergent synthetic platform, we accessed a wide variety of difluoroalkyl sulfoximine products 10–12 (65 examples, up to 77% yield), including enantiomerically pure sulfoximines. On the other hand, the formation of the radical intermediate 8 was undoubtedly proven by means of spin trapping coupled with electron paramagnetic resonance (EPR) detection. Finally, product manipulations demonstrate the usefulness of the products, including the synthesis of novel classes of cyclic F-containing sulfoximines.

## Results and discussion

We began our studies by evaluating the performance of different organophotoredox catalysts in the ATRA process between bromodifluoroalkyl sulfoximine 13 and 1-hexene 14 (Table 1). The first experiments were conducted at 20 °C, using acetonitrile as the solvent (0.5 M). Initially, we observed the formation of product 15 with the commercially available phenothiazine PC1 as well as with the dihydroacridine photocatalyst PC2 (entries 1 and 2). The NMR yield was raised up to 60% or 47%, by increasing the catalyst loading of either PC1 or PC2 from 5 to 15 mol% (entries 3 and 4). Finally, after an extensive PC screening (see ESI, Section C.1.5†), we identified

the *N*-phenyl substituted dihydroacridine PC3 as the best PC, affording the product 15 in 60% NMR yield, after 10 h (entry 5). Alongside 15, we observed the formation of byproducts arising from the radical addition of 'CF<sub>2</sub>Br radicals to 14 in variable NMR yields depending on the reaction conditions (see ESI Section C.3,† for further details). This suggests that, while C-Br bond scission predominates under these conditions, C-S bond scission is not entirely suppressed (*vide infra*).

With this result in hand, we next investigated the possibility of going beyond the classical ATRA manifold in the presence of suitable hydrogen atom transfer (HAT) donors. To our delight, the addition of 1.5 equivalent of the Hantzsch ester 17 to the previously optimized conditions mainly afforded the product 16 in 47% isolated yield, with only traces of the ATRA product 15 (entry 7). Intriguingly, the process can be promoted without the use of a PC (entry 9), indicating the pivotal excited state reactivity of the Hantzsch ester 17 under the optimized reaction conditions.<sup>11</sup> Taking into account the absorption profile of 17, we next tested other excitation wavelengths, identifying 400 nm as the most effective to obtain the hydrofunctionalization product 16 in higher yield (61% isolated yield, entry 10).

## Generality of the process

Our next efforts were directed to assess the generality of the two divergent reaction manifolds (Table 2). A wide variety of unactivated terminal alkenes 3 bearing common functionalities in medicinal chemistry settings,<sup>12</sup> including esters, ethers, silyl ethers, sulfones, boronates, or indole derivatives, were well tolerated in both reaction pathways, giving the corresponding



**Table 1** Optimization of the light-driven ATRA and hydrofunctionalization process with control experiments – selected results

Entry <sup>a</sup>	PC (mol%)	$\lambda$ (nm)	HAT donor	15 : 16 yield <sup>b</sup> (%)
1	PC1 (5)	400	—	33 : —
2	PC2 (5)	427	—	28 : —
3	PC1 (15)	400	—	60(42) : —
4	PC2 (15)	427	—	47 : —
5 <sup>c</sup>	PC3 (15)	427	—	60(52) : —
6	None	427	—	No reaction
7	PC3 (15)	427	17	5 : 51(47)
8	PC3 (15)	427	18	12 : 40
9 <sup>c</sup>	None	427	17	<5 : 55
10 <sup>c</sup>	None	400	17	— : 66(61)
11	PC3 (15)	Light off	17	No reaction

Below the table, chemical structures of PC1, PC2, PC3, and HAT donors 17 and 18 are shown.

<sup>a</sup> Reactions performed at 0.1 mmol scale, using 1 equiv. of 13 and 3 equiv of 14 (see ESI, Section C). <sup>b</sup> The yield was determined by <sup>1</sup>H-NMR analysis of the crude, using trichloroethylene as the internal standard. <sup>c</sup> Reaction time: 10 h. Isolated yields are in the parentheses.

products 19–34 in up to 68% isolated yield. As a general trend, we observed higher yields under the hydrofunctionalization conditions, in comparison with the ATRA reactivity.

Allyl chloride proved to be reactive only in the ATRA pathway, delivering the highly versatile adduct 35 in 43% yield. On the other hand, allyl-TMS successfully afforded product 36 in 53% yield under the hydrofunctionalization conditions, while desilylated alkene products are formed under the ATRA reactivity (see ESI, Section E.1†). In a similar manner, product 37 was obtained from the use of the methyl-substituted allyl-TMS under the ATRA conditions (see ESI,† for other entries) Intriguingly, the phenyl-substituted allyl-TMS proved to be only reactive in the ATRA pathway, giving the corresponding desilylated product 38 in 55% yield. Alkenes bearing pyridine or  $-\text{N}(\text{Boc})_2$  groups in terminal positions were only reactive in the hydrofunctionalization pathway, affording the products 40 and 91 (see ESI†) in 54% and 26% yield, respectively. Furthermore, inspired by previous reports,<sup>13</sup> we also synthesized the functionalized benzofuran derivative 41, *via* sequential ATRA reaction followed by a nucleophilic substitution process, starting from 2-allylphenyl acetate

(see ESI† for the synthesis of an indoline analogue). To our delight, the method proved to be amenable also to more complex biologically relevant substrates. We could use in both photochemical processes alkenes derived from  $\alpha$ -galactose, carvone,  $\beta$ -pinene, tyrosine or eugenol (42–55, see ESI Section E.1† for other entries). Alkyl and mono-fluorinated N-Ts-protected sulfoximines were also competent substrates (55 and 98). We next evaluated the scope of sulfoximines 7 in the strain-release ATRA process with [1.1.1]-propellane 9 (Table 3).<sup>14</sup> Here, likely thanks to the strain-release process, we observed higher yields, by only using 5 mol% of PC2.

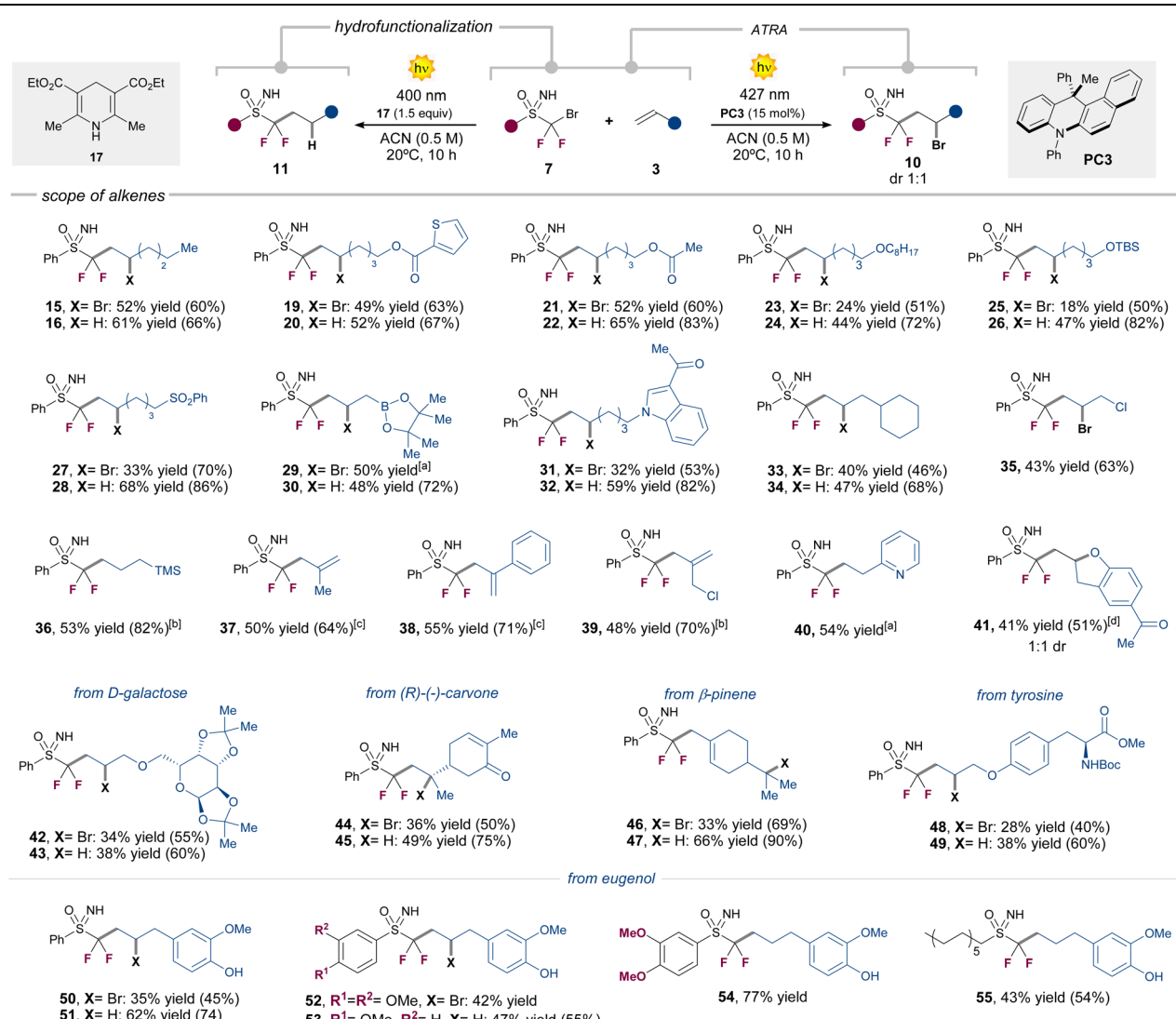
Pleasingly, different aryl and alkyl substituted N-H or N-Ts sulfoximines were successfully engaged in this transformation, affording the ATRA products 56–70 in up to 71% yield. It is worth noting that also [3.1.1]-propellanes can also be used as radical trapping agents, giving access to product 65–67 in 42–50% yield. These functionalized [3.1.1]-bicycloalkane units have been recently validated as bioisosteric replacements for *meta*-substituted arene rings, suggesting significant applications in drug design.<sup>15</sup> Although this is not the main topic of this article, it should be pointed out that a major effort has been made to prepare novel sulfoximines. In the  $\text{CF}_2\text{Br}$  series, five new sulfoximines were obtained by varying the aromatic ring on the sulfur atom (including a highly original pyridine ring). After reactions, the latter led to compounds 60 to 64. In addition, we engaged a N-Ts substituted fluorodibromo-sulfoximine in an unprecedented double sequential reduction/addition process of two [1.1.1]-propellane units, with the formation of product 70 in 42% yield. Finally, original bromo fluoromethyl sulfoximine led to the synthesis of compounds 69 and 98 (the latter described in the ESI†). We next evaluated the possibility of performing a stereospecific version of the reaction by using chiral sulfoximine precursors, while assessing the configurational stability of the radical intermediate 8 (Fig. 2a).

To this end, we submitted both enantiomers of the bromodifluoroalkyl sulfoximine 13 to the different optimized reaction conditions developed in this study. Satisfactorily, the use of either the (S)- or (R)- enantiomers of 13 led to the formation of the enantiopure ATRA products (R)-56 and (S)-56, respectively (>99.5% ee). A similar result was observed in the hydrofunctionalization pathway using eugenol 3ab as the radical acceptor (Fig. 2b). In this case, the corresponding products (R)-51 and (S)-51 were also obtained without erosion of the chirality, corroborating that the chiral difluorosulfoximine radical 8 remains configurationally stable during both photochemical processes (see ESI Section G† for further examples).

Finally, to showcase the synthetic utility of the products, we carried out a series of product manipulations (Fig. 3). First, treatment of the ATRA product 21 with NaH (60% mineral oil) in DMF allowed the deprotonation of the  $-\text{NH}$  of the sulfoximine moiety, while triggering an intramolecular cyclization process to yield the 5-membered ring sulfoximine 71 in 25% yield. It is worth mentioning that there are no other methodologies to obtain these cyclic fluorinated sulfoximines, thus demonstrating the relevance of the obtained ATRA products to access other structures of higher complexity.



**Table 2** Scope of alkenes **3** and sulfoximines **7** in the light-promoted ATRA and hydrofunctionalization reactions. Reactions performed on 0.2 mmol scale (see ESI for details). Yields refer to the isolated compounds. Values in the parentheses refer to  $^1\text{H}$ -NMR yields. If not otherwise noted dr = 1:1 (see ESI)



<sup>a</sup> Yield determined by  $^1\text{H}$ -NMR analysis from the crude reaction mixture. <sup>b</sup> Formed under hydrofunctionalization conditions. <sup>c</sup> Formed under ATRA conditions. <sup>d</sup> Reaction crude then treated with an aqueous solution of NaOH 2 M (see ESI).

Similarly, product **39** can also be treated with NaH (60% mineral oil) to induce intramolecular cyclization and yield the 6-membered ring sulfoximine **72** in 55% yield.

Furthermore, the hydrofunctionalized product **22** and the strain-released ATRA product **56** were successfully used in a copper catalyzed *N*-arylation process with phenyl iodide **73** and 3-iodopyridine **75**,<sup>16</sup> affording the *N*-phenyl substituted sulfoximine **74** and the *N*-pyridine substituted sulfoximine **76** in 87% and 50% yield, respectively.

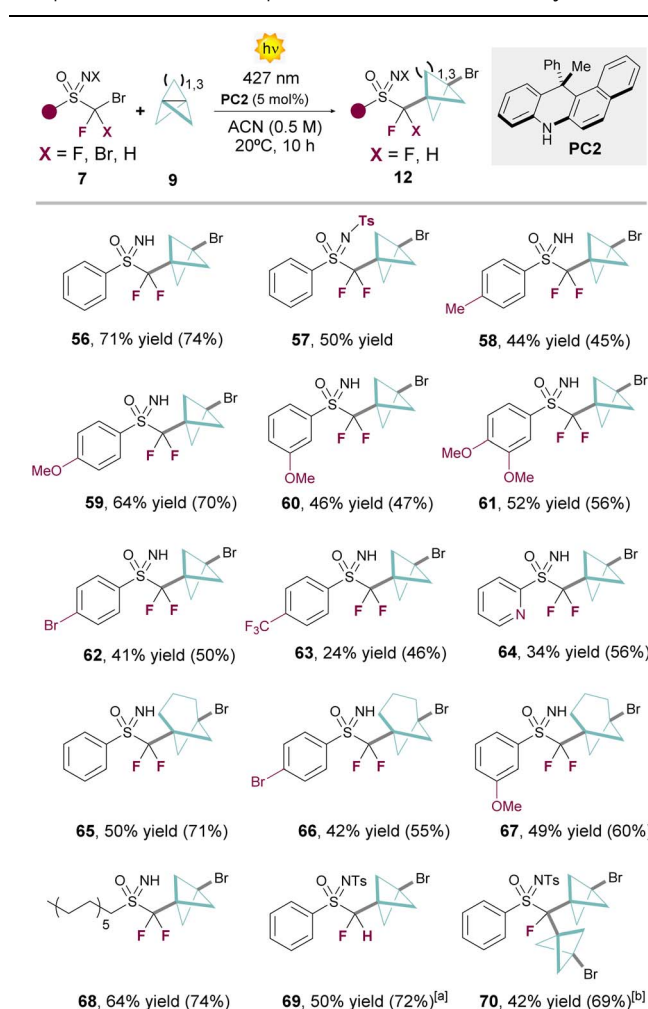
### Mechanistic investigations

We next focused on understanding the mechanisms accounting for the observed divergent reactivity. Under the

ATRA conditions, **PC3** or its EDA complex with the starting substrate (depending by the type of difluorosulfoximine used, see ESI, Section K.1† for further details) is the only absorbing species,<sup>9d</sup> whereas **17** is the main species absorbing at 400 nm in the hydrofunctionalization pathway (see ESI, Section K.1†). Stern–Volmer quenching studies showed that increasing amounts of the bromodifluoroalkyl sulfoximine **13** could effectively quench the emission of **PC3**, whereas no quenching was observed with the alkene **14** (Fig. 4a). Furthermore, the excited state redox potentials of both **PC3** and **17** [ $E_{\text{red}}(\text{PC3}^{\cdot+}/\text{PC3}^{\cdot}) = -2.30 \text{ V vs. SCE}; E_{\text{red}}(\text{17}^{\cdot+}/\text{17}^{\cdot}) = -2.28 \text{ V vs. SCE}$ ]<sup>11a,17</sup> are sufficiently negative to undergo a thermodynamically favoured SET reduction of the sulfoximine **13** [ $E_{\text{red}}(\text{13}/\text{13}^{\cdot-}) = -1.57 \text{ V vs. SCE}$ ].



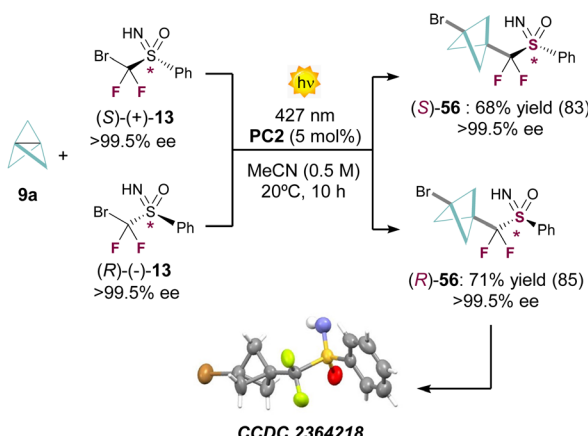
**Table 3** Scope of sulfoximines 7 that can participate in strain-release ATRA processes with propellanes 9. Yields refer to the isolated compounds. Values in the parentheses refer to  $^1\text{H}$ -NMR yields



<sup>a</sup> Reaction performed using starting material 7k (see ESI). <sup>b</sup> Reaction performed using starting material 7j (see ESI).

We next carried out a spin trapping/EPR study to detect the key difluoroalkyl radical **8a**, generated from the bromodifluoro sulfoximine **13** (Fig. 4b). A solution containing **13**, PC3 and the spin trap 2-methyl-2-nitrosopropane (**MNP**) was prepared in acetonitrile. Upon irradiation under the standard reaction conditions, the signal reported in Fig. 4b was immediately observed. Its simulation (with a virtually perfect superimposition with the red dotted line) revealed the presence of a major radical species (over 90%) whose EPR spectrum showed twelve intense lines, due to hyperfine couplings with a nitrogen nucleus ( $a_N = 11.6$  G) and two fluorine nuclei at the  $\alpha$ -position towards the nitrogen ( $a_{F1} = 22.1$  G and  $a_{F2} = 14.2$  G). On the basis of these hyperfine coupling constant (hfcc) values the spectrum recorded was assigned to the **MNP-8a** adduct of a difluorinated carbon-centered radical and was perfectly compatible with the **MNP-8a** adduct (see Fig. 4b and ESI, Section J†). Because the  $\text{CF}_2$  group was linked to a chiral sulfur atom in **8a**, the two fluorines in the spin adduct **MNP-8a** were

—(a) strain-release ATRA—



—(b) hydrofunctionalization—

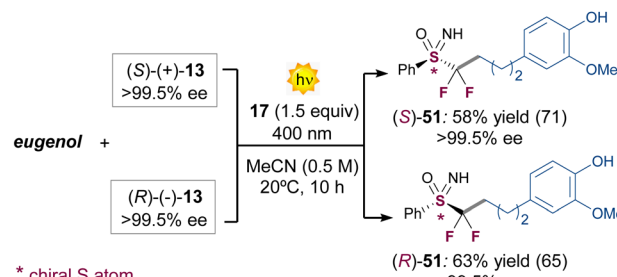
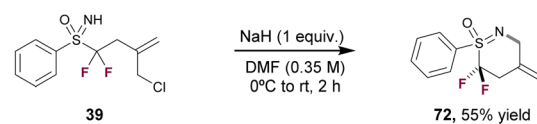
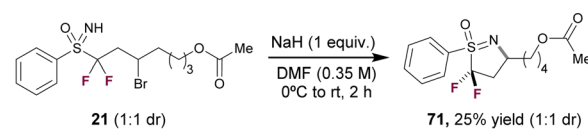


**Fig. 2** Reactions with enantiopure sulfoximines **13**; (a) ATRA reaction, and (b) hydrofunctionalization. Yields refer to the isolated compounds. Values in the parentheses refer to  $^1\text{H}$ -NMR yields.

(a) Synthesis of *F*-containing cyclic sulfoximines



(b) *N*-functionalization

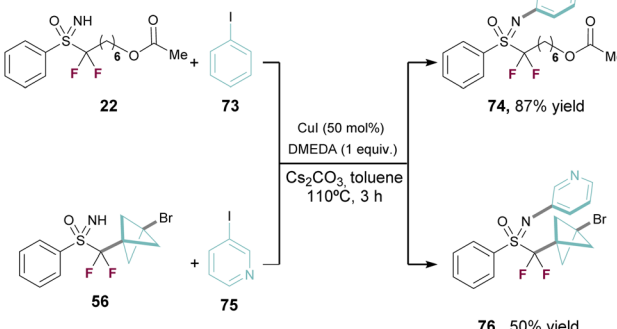


**Fig. 3** Post functionalizations of some products. (a) Synthesis of *F*-containing cyclic sulfoximines. (b) Copper-mediated *N*-functionalization. Yields refer to the isolated compounds.



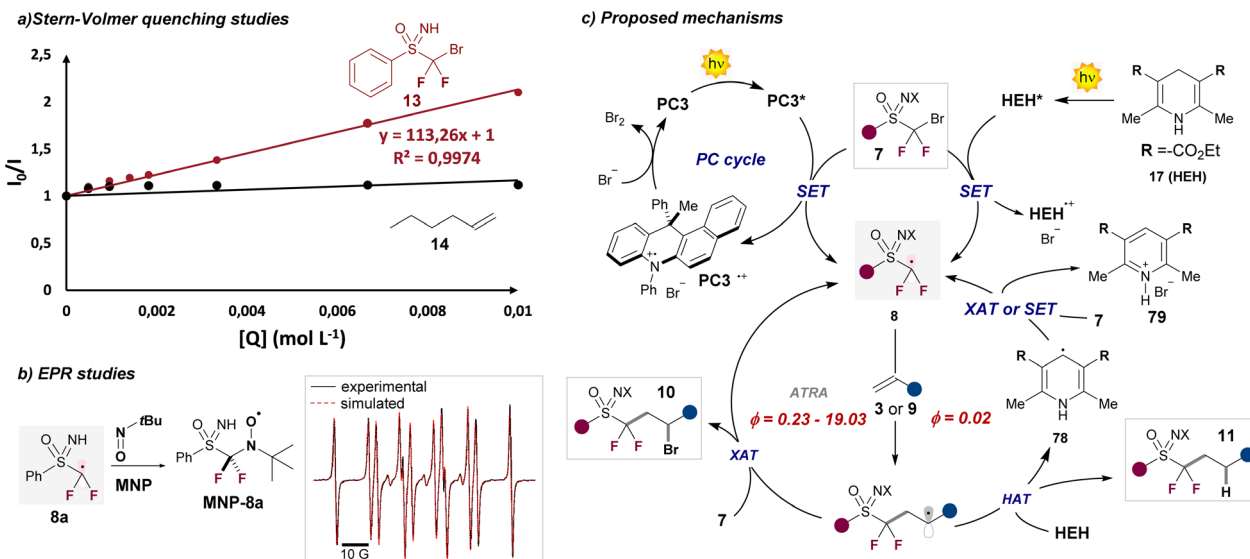


Fig. 4 (a) Stern–Volmer quenching studies. (b) EPR studies (detection key chiral radical). (c) Proposed mechanisms for the ATRA (left side) and hydrofunctionalization process (right side) developed in this study.

not magnetically equivalent, as shown by the large difference between the two hfccs. Although this phenomenon is rather common in NMR, to the best of our knowledge this is the very first description of an EPR spectrum of a radical with two non-magnetically equivalent geminal fluorine nuclei.<sup>18</sup> In addition, no EPR signal was detected before irradiation or in blank tests performed in the absence of either the substrate 13 or PC3.

Based on these experimental findings, we propose the divergent mechanism illustrated in Fig. 4c. On one hand, the ATRA pathway is initiated by a photoinduced SET process from the excited PC3\* to sulfoxime 7, producing the difluorosulfoxime radical 8 and the radical cation of the photocatalyst (PC3<sup>+</sup>). The open-shell intermediate 8 participates in a radical addition process to alkene 3 (the same ATRA manifold with propellane 9 has been omitted for clarity), forming the intermediate 88. This radical (88) undergoes halogen atom transfer (XAT) with another molecule of sulfoxime 7, affording the ATRA product 10 along with the reactive radical 8. This chain propagation mechanism is supported by a relatively high quantum yield value of  $\phi = 0.23$  for 3 and 19.03 for 9. On the other hand, the hydrofunctionalization reaction is initiated by a photoinduced SET process from the excited Hantzsch ester 17\* to 7, delivering the key radical 8 and the radical cation of HEH<sup>+</sup>.<sup>17</sup> In this scenario, the intermediate 77 formed after the radical addition undergoes a HAT process with another molecule of HEH to afford the desired product 11, alongside radical 78. Most likely, the rate of the HAT is faster than the XAT, thereby explaining the preferential formation of product 11 over 10. The very low quantum yield value registered for this process ( $\phi = 0.02$ ) suggests the activity of an in-cage mechanism. However, at the current stage we cannot exclude the operation of a very inefficient chain propagation mechanism, in which the radical 78 reduces 7, generating another reactive radical 8 and the Hantzsch pyridinium 79.<sup>19</sup>

## Conclusions

In conclusion, we have developed a divergent synthetic platform for the efficient installation of valuable fluorinated sulfoximine moieties onto olefins and bicycloalkanes.<sup>20</sup> Interestingly, by the rational selection of the reducing agent, either the excited PC3 or the Hantzsch ester 17, it is possible to channel the chemistry towards Br- or the H-containing fluorinated sulfoximine product, respectively. We have shown the generality of these processes with diverse classes of molecules, including olefins and propellanes bearing a large variety of functional groups (65 examples, up to 77% yield). Further, it was possible to transfer chiral sulfoximine radicals with complete stereoretention into the final products. Finally, we performed a series of product manipulations accessing structurally relevant synthetic targets such as cyclic 71 and 72. Mechanistic investigations revealed the key activity of the fluorinated radical 8 (characterized by EPR) that undergoes ATRA or hydrofunctionalization pathways.

## Data availability

The data supporting this article have been included as part of the ESI.<sup>†</sup>

## Author contributions

S. C., L. D. and E. M. conceived and directed the project. S. B., S. C., J. P., E. A., and G. D. performed the experiments and prepared the starting materials. S. B., S. C., J. P., and E. A. characterized the products and intermediates. B. T. performed the EPR analysis. G. P. performed the X-ray analysis. S. C., L. D. and E. M. wrote the manuscript with contributions from all the authors.

## Conflicts of interest

There are no conflicts to declare.

## Acknowledgements

This work was supported by MUR (Ministero dell'Università PRIN2022PNRR23\_01 (L. D.), and (European Research Council) ERC-Starting Grant 2021 SYNPHOCAT 101040025 (L. D.). The authors gratefully acknowledge the technical support units at the Department of Chemical Sciences (DiSC) of the University of Padova, in particular Dr Ilaria Fortunati, Samuel Pressi and Stefano Mercanzin. B. T. acknowledges the NIEHS for providing free public electron paramagnetic resonance software tools (Winsim simulation program and spin trap database). S. B. acknowledges UniPD for a doctoral fellowship. J. P. thanks the University of Paris-Saclay and the University of Padova for financial support *via* the grant BorsaDISC27 and Paris-Saclay grant as an international cotutelle collaboration. Dr Nicolas Vanthuyne (Aix Marseille Université, CNRS, UMR 7313-iSm2) is acknowledged for the preparative HPLC separation of the enantiomers of the sulfoximine 13.

## References

- (a) C. R Johnson, *Comprehensive Organic Chemistry*, 1st edn, 1979, vol. 3, p. 223; (b) M. Reggelin and C. Zur, *Synthesis*, 2000, **1**, 1; (c) S. G. Pyne, *Sulfur Rep.*, 1999, **21**, 281; (d) M. Frings, C. Bolm, A. Blum and C. Gnamm, *Eur. J. Med. Chem.*, 2017, **126**, 225; (e) U. Lücking, *Angew. Chem., Int. Ed.*, 2013, **52**, 9399; (f) Y. Han, K. Xing, J. Zhang, T. Tong, Y. Shi, H. Cao, H. Yu, Y. Zhang, D. Liu and L. Zhao, *Eur. J. Med. Chem.*, 2021, **209**, 112885; (g) P. Mäder and L. Kattner, *J. Med. Chem.*, 2020, **63**, 14243; (h) U. Lücking, *Org. Chem. Front.*, 2019, **6**, 1319; (i) E. Boulard, V. Zibulski, L. Oertel, P. Lienau, M. Schäfer, U. Ganzer and U. Lücking, *Chem. Eur. J.*, 2020, **26**, 4378; (j) U. Lücking, *Chem. Eur. J.*, 2022, **28**, e202201993. For selected recent examples, see: ; (k) S. Teng, Z. P. Schultz, C. Shan, L. Wojtas and J. M. Lopchuk, *Nat. Chem.*, 2024, **16**, 183; (l) M. D. Glossbrenner, S. González-Granda, O. S. Nayal, E. A. Noten, C. M. Balintfy, D. A. Pratt and C. R. J. Stephenson, *ChemRxiv*, 2023, preprint, DOI: [10.26434/chemrxiv-2023-gw0xb](https://doi.org/10.26434/chemrxiv-2023-gw0xb); (m) Z. Zhong, B. J. W. Hocking, C. P. Brown, T.-K. Ma, A. J. P. White, D. J. Mann, A. Armstrong and J. A. Bull, *Angew. Chem., Int. Ed.*, 2024, e202420028; (n) N. S. Greenwood, Z. W. Boyer, J. A. Ellman and C. Gnamm, *J. Med. Chem.*, 2025, **68**, 4079.
- E. Anselmi, B. Montigny, M. Lökov, C. Keskula, J. E. Soosaar, S. Tshepelevitsh, T. Billard, E. Magnier and I. Leito, *Chem. Eur. J.*, 2025, **31**, e202402329.
- Selected reviews: (a) S. Purser, P. R. Moore, S. Swallow and V. Gouverneur, *Chem. Soc. Rev.*, 2008, **37**, 320; (b) D. O'Hagan, *J. Fluorine Chem.*, 2010, **131**, 1071; (c) J. Wang, M. Sánchez-Roselló, J. L. Aceña, C. Del Pozo, A. E. Sorochinsky, S. Fustero, V. A. Soloshonok and H. Liu, *Chem. Rev.*, 2014, **114**, 2432; (d) V. Bizet and D. Cahard, *Chem. Soc. Rev.*, 2014, **43**, 135; (e) H. Mei, J. Han, S. Fustero, M. Medio-Simon, D. M. Sedgwick, C. Santi, R. Ruzziconi and V. A. Soloshonok, *Chem. Eur. J.*, 2019, **25**, 11797; (f) M. Inoue, Y. Sumii and N. Shibata, *ACS Omega*, 2020, **5**, 10633.
- For selected reviews, see: (a) M. Andresini, A. Tota, L. Degennaro, J. A. Bull and R. Luisi, *Chem. Eur. J.*, 2021, **27**, 17293; (b) V. Bizet, R. Kowalczyk and C. Bolm, *Chem. Soc. Rev.*, 2014, **43**, 2426; (c) X. Shen and J. Hu, *Eur. J. Org. Chem.*, 2014, 4437, For selected examples of bioactive fluorinated sulfoximines, see: ; (d) Y. Zhu, R. B. Rogers and J. X. Huang, *US Pat.*, US 20050228027, 2005; (e) A. Plant, J. E. Boehmer and A. L. Peace, *GB Pat.*, WO 2006037945, 2006; (f) M. Haerter, H. Beck, P. Ellinghaus, K. Berhoerster, S. Greschat, K.-H. Thierauch and F. Suessmeier, *German Pat.*, WO 2010054764, 2010.
- (a) S. Chaabouni, J.-F. Lohier, A.-L. Barthelemy, T. Glachet, E. Anselmi, G. Dagousset, P. Diter, B. Pégot, E. Magnier and V. Reboul, *Chem. Eur. J.*, 2018, **64**, 17006; (b) A.-L. Barthelemy, V. Cortal, G. Dagousset, E. Anselmi, L. Bertin, L. Fabien, B. Salgues, P. Courtes, C. Poma, Y. El-Ahmad and E. Magnier, *Org. Process Res. Dev.*, 2020, **24**, 704; (c) E. Magnier, *Emerging Fluorinated Motifs: Synthesis, Properties, and Applications*, 2020, vol. 2, 675; (d) A.-L. Barthelemy and E. Magnier, *C. R. Chim.*, 2018, **21**, 711.
- (a) C. K. Prier, D. A. Rankic and D. W. MacMillan, *Chem. Rev.*, 2013, **113**, 5322; (b) N. A. Romero and D. A. Nicewicz, *Chem. Rev.*, 2016, **116**, 10075; (c) M. H. Shaw, J. Twilton and D. W. MacMillan, *J. Org. Chem.*, 2016, **81**, 6898.
- (a) T. Koike, *Chem. Rec.*, 2023, **23**, e202300032; (b) M. Briand, L. D. Thai, F. Bourdrex, N. Vanthuyne, X. Moreau, E. Magnier, E. Anselmi and G. Dagousset, *Org. Lett.*, 2022, **24**, 9375; (c) T. Duhail, S. Messaoudi, G. Dagousset, J. Marrot, C. André-Barrès, E. Magnier and E. Anselmi, *Adv. Synth. Catal.*, 2023, **365**, 2392.
- A. Prieto, P. Diter, M. Toffano, J. Hannedouche and E. Magnier, *Adv. Synth. Catal.*, 2019, **361**, 436.
- (a) N. Erdeljac, K. Bussmann, A. Schöler, F. K. Hansen and R. Gilmour, *ACS Med. Chem. Lett.*, 2019, **10**, 1336; (b) S. Meyer, J. Häfliiger and R. Gilmour, *Chem. Sci.*, 2021, **12**, 10686; (c) Y. Kraemer, C. Ghiazza, A. N. Ragan, S. Ni, S. Lutz, E. K. Neumann, J. C. Fettinger, N. Nöthling, R. Goddard and J. Cornella, *Angew. Chem., Int. Ed.*, 2022, **61**, e202211892; (d) S. Cuadros, G. Goti, G. Barison, A. Raulli, T. Bortolato, G. Pelosi, P. Costa and L. Dell'Amico, *Angew. Chem., Int. Ed.*, 2023, **62**, e202303585.
- While various difluoroalkylating agents, including sulfone derivatives such as  $\text{BrCF}_2\text{-SO}_2\text{Ph}$ , have been used for the incorporation of difluoroalkyl moieties into organic compounds, no radical ATRA or hydrofunctionalization processes have been developed with the corresponding difluoroalkylsulfoximines. For recent reviews on difluoroalkylations, see: (a) S. Barata-Vallejo and A. Postigo, *Molecules*, 2019, **24**, 4483; (b) A. Lemos, C. Lemaire, A. Luxen and A. Synt, *Adv. Synth. Catal.*, 2019, **361**, 1500; (c) R. Jia, X. Wang and J. Hu, *Tetrahedron Lett.*, 2021, **75**, 153182; (d) J. Sheng, K.-J. Bian, Y.-M. Su,



G.-X. Liao, R. Duan, C. Li, Z. Liu and X.-S. Wang, *Org. Chem. Front.*, 2020, **7**, 617.

11 (a) P.-Z. Wang, J.-R. Chen and W.-J. Xiao, *Org. Biomol. Chem.*, 2019, **17**, 6936; (b) X. Huang, S. Luo, O. Burghaus, R. D. Webster, K. Harms and E. Meggers, *Chem. Sci.*, 2017, **8**, 7126; (c) H. Yan, Y. Liu, X. Feng and L. Shi, *Org. Lett.*, 2023, **25**, 8116.

12 P. Ertl, E. Altmann and J. M. McKenna, *J. Med. Chem.*, 2020, **63**, 8408.

13 V. Corti, J. Dosso, M. Prato and G. Filippini, *J. Org. Chem.*, 2023, **88**, 6008.

14 (a) K. B. Wiberg, S. T. Waddell and K. Laidig, *Tetrahedron Lett.*, 1986, **27**, 1553; (b) P. Bellotti and F. Glorius, *J. Am. Chem. Soc.*, 2023, **145**, 20716; (c) S. Cuadros, J. Paut, E. Anselmi, G. Dagousset, E. Magnier and L. Dell'Amico, *Angew. Chem., Int. Ed.*, 2024, e202317333.

15 (a) N. Frank, J. Nugent, B. R. Shire, H. D. Pickford, P. Rabe, A. J. Sterling, T. Zarganes-Tzitzikas, T. Grimes, A. L. Thompson, R. C. Smith, C. J. Chofield, P. E. Brennan, F. Duarte and E. A. Anderson, *Nature*, 2022, **611**, 721; (b) T. Iida, J. Kanazawa, T. Matsunaga, K. Miyamoto, K. Hirano and M. Uchiyama, *J. Am. Chem. Soc.*, 2022, **144**, 21848.

16 Y. Macé, B. Pégot, R. Guillot, C. Bournaud, M. Toffano, G. Vo-Thanh and E. Magnier, *Tetrahedron*, 2011, **67**, 7575.

17 G. S. Yedase, S. Venugopal, P. Arya and V. R. Yatham, *Asian J. Org. Chem.*, 2022, **11**, e202200478.

18 D. R. Duling, *J. Magn. Reson., Ser. B*, 1994, **104**(2), 105.

19 M. A. Cismesia and T. P. Yoon, *Chem. Sci.*, 2015, **6**, 5426.

20 S. Baldon, L. Dell'Amico and S. Cuadros, *Eur. J. Org. Chem.*, 2024, e202400604.

